JOURNAL OF CATALYSIS 109, 396–406 (1988)

Experimental Procedures for the Analysis of Intraparticle Diffusion during Temperature-Programmed Desorption from Porous Catalysts in a Flow System

Y.-J. HUANG, J. XUE, AND J. A. SCHWARZ[1]

Department of Chemical Engineering and Materials Science, Syracuse University, Syracuse, New York 13244

Received March 11, 1987; revised August 20, 1987

An analog to the Weisz–Prater method is used to analyze the effect of intraparticle diffusion under the nonisothermal conditions of a temperature-programmed desorption (TPD) experiment. By taking into account the temperature-dependent transport properties and the readsorption of the adsorbate, the importance of intraparticle mass transfer during TPD is assessed by the magnitude of the effectiveness factor η. Experimental TPD spectra of CO and H_2 from Ni/SiO_2 catalysts serve as prototype examples for desorption of these adsorbates from Group VIII supported metal catalysts. It is found that the observed desorption rate, particle size, surface concentration of the adsorbate, effective diffusivity of the adsorbate in the carrier gas/catalyst particle, catalyst bed volume, heating rate, and initial surface coverage of the adsorbate collectively determine the magnitude of the effectiveness factor. Characteristic plots for first- and second-order desorption, respectively, are presented to guide the experimentalist in selecting the appropriate experimental parameters to minimize the effect of intraparticle gradients during the TPD process.

INTRODUCTION

The importance of mass transfer limitations within a catalyst pellet under reaction conditions has traditionally been analyzed in terms of a diffusion factor (*1*) and a modulus (*1*) which depend upon both the geometry of the particle and the reaction order (*2*). Although these considerations have been applied primarily to a static system they also apply to a flow reactor (*1*). In a flow system it is assumed that a steady state in the concentration gradient results from local diffusion in a volume element of gas and the catalyst surface. This is equivalent to a slug of gas volume which moves through the catalyst bed and samples the catalyst for a period of its residence time in the bed. These conditions are met by the small beds and high carrier gas flow rates used in a TPD experiment (*3*).

The existence of intraparticle mass transfer effects was addressed experimentally by Lee *et al.* (*4, 5*). A series of TPD experiments was carried out at constant heating rate and carrier gas flow rate with H_2 and CO as adsorbates. The peak temperatures did not shift as the particle size was increased by more than a factor of 10 (22–500 μm). Furthermore, the order of the desorption kinetics, corrected for readsorption (*4, 5*) of CO and H_2, was found to be 1 and 2, respectively. Collectively, these results strongly suggested that intraparticle diffusion was not a dominant mass transfer effect (*1*) in their TPD experiments.

In order to provide adequate criteria to confirm the absence of intraparticle gradients, we reexamine here the effect of mass transfer *during* TPD for *both* first- and second-order desorption from porous catalysts to determine under what conditions intraparticle diffusion will not confound the interpretation of TPD spectra to obtain ki-

[1] To whom correspondence should be addressed.

0021-9517/88 $3.00

netic parameters. Experimental results for hydrogen and carbon monoxide as adsorbates and a commonly used carrier gas have been considered in this analysis. What emerges is that a single criterion as proposed in earlier investigations (*1, 3, 6, 7*) is replaced by regions of characteristic plots because the parameters that comprise these plots are temperature dependent. The objective of this report is, therefore, to demonstrate the procedures that can be employed to analyze the aforementioned characteristic plots and thus allow the experimentalist to assess the extent of intraparticle gradients due to conditions existing *during* the TPD experiment.

We will demonstrate that the existence and magnitude of a diffusion effect are entirely determined by the magnitude of a pseudo-modulus which involves the particle size, bed volume, effective diffusivity, the measured desorption rate, and a concentration term. We will consider spherical particles and first-order (CO desorption) and second-order (H_2 desorption) reactions. In many experimental cases the intrinsic rate constant will not be directly known, but instead it will be desirable to estimate the pseudo-modulus from the diffusivity, the actually observed desorption rate, bed volume, and the size of catalyst particle. In a TPD experiment the first two quantities will vary during the temperature ramp and a suitable method is required to ensure that for a given adsorbate/carrier gas system, the experimental parameters (such as particle size and surface concentration of the adsorbate) are selected to avoid internal concentration gradients over the entire temperature range where desorption is measurable.

ANALYSIS OF DIFFUSION EFFECTS

Under steady-state operating conditions, diffusion and chemical reaction occur simultaneously within a porous particle. If the diffusion of reactant *into* the particle is rapid compared to the reaction rate, the entire internal surface area within the catalyst particle is effectively accessed by the reactant and this results in a uniform reactant concentration profile throughout the catalyst particle. As a consequence, the whole catalyst surface (both external and internal) is very effective in promoting the reaction. If, on the other hand, the diffusion rate into the catalyst particle is slower than the reaction rate, a concentration gradient occurs within the catalyst particle. Within the center core of the catalyst particle, the reactant concentration is substantially lower than the reactant concentration at the periphery of the particle. Most of the reaction, therefore, takes place within a thin shell on the periphery of the catalyst particle, and the internal surface is not used effectively. In order to determine how effectively the catalyst surface is used under reaction conditions, an effectiveness factor, η, was introduced by Weisz and Prater (*1*). It is defined as the ratio of the observed reaction rate to that rate observed if the total surface area throughout the catalyst particle were exposed to the same environment found at the outer surface. In other words, Weisz and Prater proposed that under *isothermal* conditions the effect of intraparticle diffusion can be contained in a separate factor, η, in the general rate equation

$$R = kV_c C_0^n \eta, \tag{1}$$

where R is the observed reaction rate (mol/s), V_c is the bed volume (cm^3), C_0 is the concentration of the reactant at the particle's surface (mol/cm^3), and n is the order of the reaction. The reaction rate constant, k, has units of $(\text{concentration})^{1-n}\ s^{-1}$. For a spherical catalyst particle of radius r_s the diffusion modulus can be written for the general case described by Eq. (1) as

$$\phi_s = \frac{r_s}{3}\left[\frac{kC_0^{n-1}}{D_{\text{eff}}}\right]^{1/2}. \tag{2}$$

In Eq. (2), D_{eff} is the effective diffusion coefficient characterizing the ability for diffusive flow through a unit geometric volume of the solid particle.

It is important to note that the reference point of Eqs. (1) and (2) is chosen at the outer surface of the particle. For a reaction in which the reactant is supplied by the outside environment, the external surface has a higher concentration than at the center. The choice of the outer surface as the reference point, to calculate η, ensures that the value of η is between 0 and 1.

The appropriate representation for the reaction rate during a TPD process requires simultaneous consideration of the adsorption rate and the desorption rate of the adsorbate. If for a narrow range of temperature change, the nonsteady term in the materials balance for the adsorbate is small compared to the average adsorbate concentration in the particle, then it is reasonable to treat the system as if it were in the quasi-steady state. This would be expected by simple analysis of the TPD spectrum. At any temperature for which the desorption rate is measured, the corresponding concentration of the adsorbate in the particles can be assessed by the procedure to be outlined shortly. It has been demonstrated experimentally (5) and by numerical simulation (6) that equilibrium adsorption is very closely approximated throughout the course of TPD. This observation has motivated the following extension of the traditional formulation proposed by Weisz and Prater.

When readsorption is considered, the observed rate R to account for adsorption equilibrium *during a TPD process* is

$$R = [k_d C_i^n - k_a P_a (C_m - C_i)^n] V_c \eta, \quad (3)$$

where k_a and k_d are the specific rate constants for adsorption and desorption, P_a is the gas phase pressure of the adsorbate, C_m is the density of sites accessible for adsorption, C_i is the adsorbate concentration at the center of the particle, and the term $(C_m - C_i)^n$ describes the concentration of vacant adsorption sites. It is important to note that the center of the particle is chosen as the reference point to calculate the effectiveness factor η for a *desorption process*. The reactant (i.e., adsorbate) during TPD is supplied by the reservoir inside the particle and it diffuses *outward* through the particle. Because the center will have a higher adsorbate concentration than the outer surface, choosing the center of the particle as the reference point to calculate η will ensure that the value of η calculated is between 0 and 1, and thus the "TPD reaction" can be modeled by procedures developed by Weisz and Prater.

An adsorption/desorption ratio K is introduced to simplify Eq. (3):

$$K = \frac{k_a P_a (C_m - C_i)^n}{k_d C_i^n} \quad (4)$$

Substituting Eq. (3) into Eq. (4) we recover an equation whose form is similar to that of Eq. (1), i.e.,

$$R = (1 - K) k_d V_c C_i^n \eta = k_{eff} V_c C_i^n \eta. \quad (5)$$

The effective desorption rate (k_{eff}) for the case of readsorption is given by $(1 - K)k_d$. We write Eq. (5) by analogy to Eq. (1) to simplify the discussion to follow. In actuality, k_{eff} has no physical significance.

A modulus, ϕ_s, for the desorption reaction described in Eq. (5) can be constructed by the same method used by Weisz and Prater as

$$\phi_s = \frac{r_s}{3} \left[\frac{k_{eff} C_i^{n-1}}{D_{eff}} \right]^{1/2}. \quad (6)$$

The magnitude of ϕ_s is used to estimate the effectiveness factor, η, which in turn provides a measure of the ratio of the actual rate for the catalyst particle to the maximum rate which is evaluated at the center of the particle. In other words η is a measure of the concentration gradient of the reactant within the particle.

The analysis of diffusion effects during a TPD experiment is complicated by several factors. The kinetic parameters which determine the magnitude of the rate constant are generally not known. The transport properties of the gas phase species are temperature dependent and will change with

the increase in temperature during the experiment. In order to simplify the evaluation of ϕ_s a pseudo-modulus can be constructed by combining Eqs. (5) and (6) to eliminate k_{eff}. The result for nth-order kinetics is

$$9\eta\phi_s^2 C_i = \frac{r_s^2 R}{D_{eff} V_c}. \qquad (7)$$

The left hand side of Eq. (7) was determined numerically for a spherical catalyst particle by solving the appropriate mass balance equation at closely spaced temperatures over a range appropriate to a TPD experiment. The numerical procedures, described in the Appendix, are justified on the basis that it has been found from model predictions (*3, 6, 8*) that adsorption equilibrium is closely approached throughout the catalyst bed during the TPD process. Thus at any time during the TPD experiment, the unsteady-state problem can be solved using a steady-state approximation. In this form the results of the calculation depend on C_i. However, C_s, the average adsorbate concentration in the particles, is the quantity determined experimentally. Hence we designate ϕ_s as a pseudo-modulus. To provide the necessary "bridge" between experiment and numerical simulation the adsorbate concentration profile within the catalyst particle (obtained numerically) can be integrated throughout the particle by the procedures described in the Appendix to yield the average adsorbate concentration in the particle, C_s.

The η–ϕ_s calculations for steady-state reaction systems have been performed by Weisz and Prater (*1*). The direct application of their results to a TPD process in which the temperature is not constant yields results that are not presented in a way in which all the parameters can be experimentally determined during a TPD process. For example, the quantity C_s at any temperature (or time) can be determined experimentally. The value of C_s is obtained from the TPD spectrum at any temperature by evaluating the area under the TPD curve from the selected temperature to a temperature high enough that desorption has ceased. The ratio of this area to the total area times C_m yields the value of C_s. It is interesting to note that the ratios of the measured desorption rate per unit volume to the value of C_s for the examples treated in the next section are $\sim 10^{-3}$ for second-order and $\sim 10^{-4}$ for first-order desorption which further substantiates treating this nonsteady-state problem by a steady-state model.

Figures 1a and 1b are characteristic plots for evaluating diffusion effects in porous spherical catalyst particles during a TPD experiment for $n = 1$ and 2, respectively. The ordinate, η, is the effectiveness factor which is a measure of the concentration gradient within the particle. If $\eta = 1$ the concentration is uniform. The abscissa is comprised of terms that can be controlled in the experiment (r_s, V_c), estimated by correlations (*9*) (D_{eff}), or measured during the TPD experiment at any temperature (R). The value of C_s at any temperature can be determined once a value of C_m is obtained; C_m is the maximum number of adsorption sites and can be measured by, e.g., pulsed or static selective chemisorption of the adsorbate. The range of the abscissa was obtained by considering the following typical TPD experimental parameters: R (5×10^{-8}–5×10^{-7} mol/s), r_s (1×10^{-2}–0.5 cm), D_{eff} (1×10^{-3}–1×10^{-1} cm^2/s), and V_c (0.1–1.0 cm^3).

THE PSEUDO-MODULUS

Direct application of Figs. 1a and 1b to assess mass transfer effects requires further discussion. The traditional variable that can be controlled by the experimentalist to minimize concentration gradients within a catalyst particle is its average size. It should be noted that choice of particle size determines the volume of catalyst required for adequate sensitivity in detection of the adsorbate during desorption. Furthermore, the upper bound of the minimum particle size should govern the experimental choice

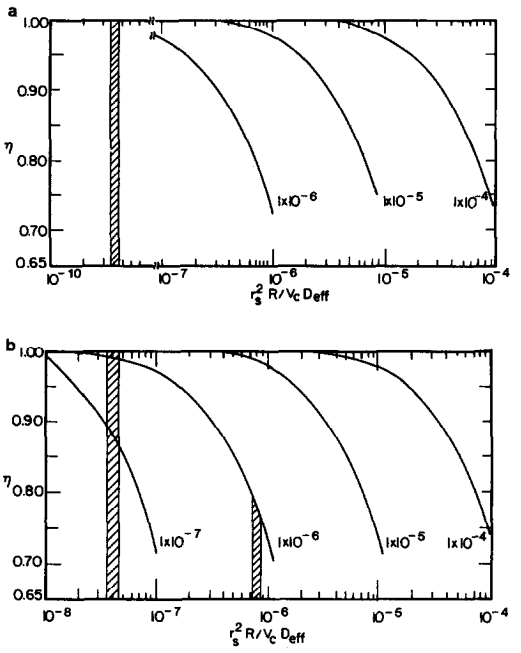

FIG. 1. Characteristic plots of effectiveness factor, η, vs Rr_s^2/V_cD_{eff} parametric in surface concentration of adsorbate for (a) first-order and (b) second-order desorptions, respectively.

of particle size to avoid excessive pressure drop across the catalyst bed (*10*).

The transport properties of the gas phase species are temperature dependent and will increase with increasing temperature; the magnitude will also depend upon the binary gas/adsorbate/carrier gas system employed. Table 1 lists calculated transport parameters at selected temperatures. Values of D_m, the molecular diffusivity, for the binary gas systems CO/He and H_2/He have been evaluated from various correlations (*11–14*). Lower and upper bounds were found to depend on the correlation chosen.

TABLE 1

The Effect of Increasing Temperature on D_{eff}, R, θ, C_s, r_s^2R/V_cD_{eff}, and η

Order of desorption	Second order			First order		
Adsorbate	H_2			CO		
Carrier gas	He			He		
Weight of catalyst (g)	0.1			0.1		
Particle size (cm)	0.0225			0.003		
Bed volume (cm^3)	0.139			0.105		
Temperature (K)	400	500	600	500	600	700
D_{eff}^{+} (10^{-3} cm^2/s)	3.4	3.8	4.2	1.0	1.1	1.2
D_{eff}^{++} (10^{-3} cm^2/s)	3.9	4.4	4.8	1.2	1.3	1.4
R (10^{-7} mol/s)	0.30	1.32	0.78	0.16	0.15	0.11
θ	0.98	0.50	0.24	0.69	0.47	0.19
C_s (10^{-4} mol/cm^3)	4.70	2.40	1.15	6.26	4.27	1.72
Rr_s^2/V_cD_{eff} (10^{-8} cm^3/mol)	0.81	3.19	1.71	0.031	0.027	0.018
η		>0.99			>0.99	

The results we report are based on the mean values for each gas mixture determined at 298 K. The temperature dependence ($\sim T^{1/2}$) is the same regardless of the correlation used to evaluate D_m (*15*). There is no unique way to evaluate the effective diffusivity (*8*); we report two ways to calculate this quantity (*9*).

The value of the pseudo-modulus is also dependent on the magnitude of the observed desorption rate, R. The magnitude of R at any time (or temperature) during TPD will depend on the experimental conditions. For example, the experimentalist can control the carrier gas flow rate over a reasonable range (20–200 cc/min) while still maintaining adequate detection sensitivity; the magnitude of the carrier gas flow rate affects the measured desorption rate. The heating rate, which also affects signal sensitivity and the measured desorption rate, can also be varied.

The pseudo-modulus is parametric in C_s, the average concentration of the adsorbate in the particle which varies continuously during the desorption process. The effect of C_s on η depends on the order of the desorption kinetics and this effect is reflected in Fig. 1 which was determined by solving the continuity equation for the spherical geometry and $n = 1$ or 2 parametric in C_s. The range in values of C_s was chosen to be consistent with typical metal surface areas determined by selective chemisorption of each of the adsorbates, H_2 or CO. The temperature-dependent magnitude of D_{eff}, R, and C_s (at a given r_s and V_c) collectively determines the magnitude of effectiveness factor.

The results shown in Figs. 1a and 1b allow the experimentalist to assess the impact of mass transfer effects and to adjust experimental conditions so that $\eta \rightarrow 1$ and thus the TPD data can be directly analyzed to determine the desorption kinetic parameters by procedures described elsewhere (*4, 5*). To demonstrate the application of the results shown in Figs. 1a and 1b we will consider laboratory data for the desorption of H_2 and CO in a He carrier gas from nickel supported on silica catalysts. Table 2 presents a summary of catalyst and bed properties used in the experimental study.

TABLE 2

Summary of Catalyst and Bed Properties Used in the Experimental Study (*4, 5*) and Calculated Transport Parameters at Selected Temperatures for First-Order and Second-Order Desorption of CO and H_2 in a He Carrier Gas, Respectively

Adsorbate	H_2	CO
Carrier gas	He	He
Flow rate (cm^3/min)	100	100
Weight of catalyst (gm)	0.1	0.1
Particle size (cm)	0.0225	0.003
Bed volume (cm^3)	0.139	0.105
Bed void fraction	0.54	0.40
Initial coverage	0.7	1.0
Bed length (mm)	5.0	5.0

APPLICATIONS

First-Order Desorption of CO

Figure 2a is a TPD spectrum of CO desorption (from an initial saturation coverage) from Ni/SiO_2 (*4*). For further clarification Fig. 2b shows the surface phase CO profile down the axial length of the bed during TPD from a saturated surface determined by the simulation of Lee *et al.* (*4*). The profile is nearly uniform indicating the absence of axial dispersion in the shallow catalyst bed used in TPD, and thus a nearly uniform concentration throughout the bed exists. This is unlike the situation in a packed bed which produces more uniform axial concentration profiles. In those cases steeper concentration profiles can exist even in the absence of axial dispersion compared to those in the presence of axial dispersion.

CO desorption from an initially saturated surface is required to ensure uniformity in the axial surface phase concentration (*5*). When allowance is made for repulsive interactions between adsorbates, it is found that significant redistribution of the adsorbate within the bed occurs. This results

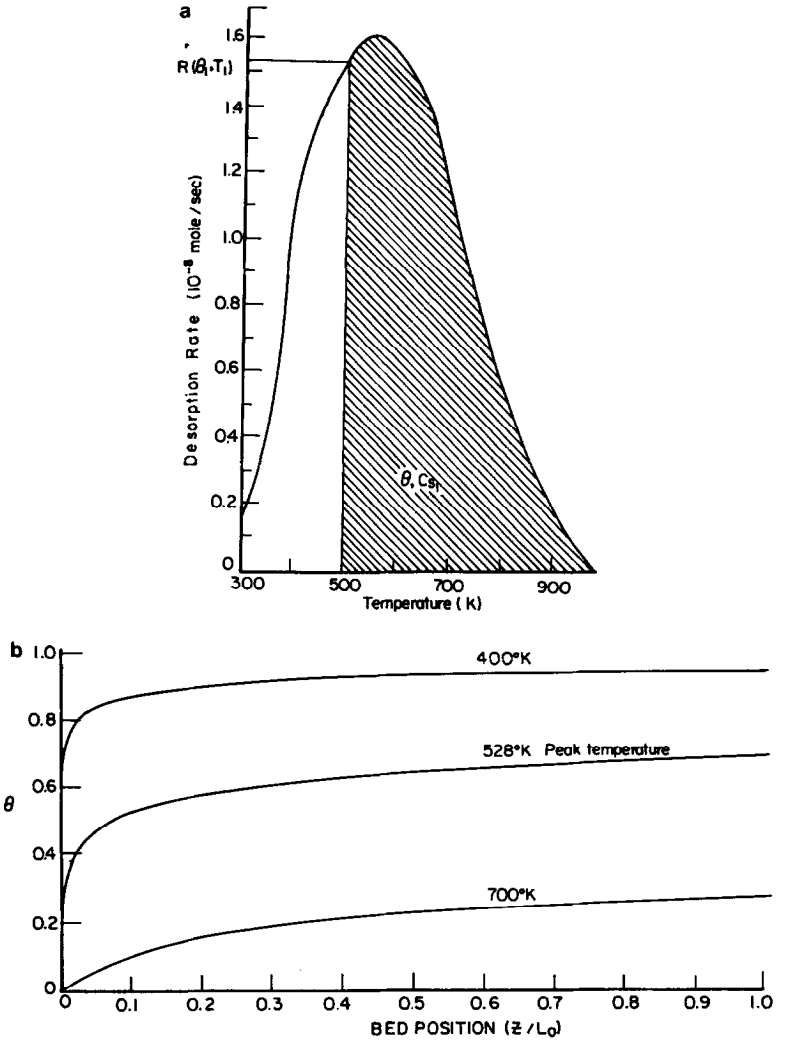

FIG. 2. (a) Experimental TPD spectrum of CO from an initial saturated surface of Ni/SiO_2 and (b) the surface phase CO profile down the axial length of the bed during TPD (*5*).

in nearly uniform adsorbate profiles which are obtained when experimental conditions are selected properly. Furthermore, "annealing" in the concentration gradient during TPD with increasing temperature was reported before (*6*) for H_2 and CO desorption under conditions representative of those used in experiments with supported Group VIII metals.

The experimental conditions and catalyst properties required to evaluate the pseudo-modulus and C_s are given in Table 1. We choose three temperatures (500, 600, and 700 K) to determine characteristic parameter values below, at, and above the peak temperature maximum. The pertinent values at each temperature are given in Table 2. The value of the abscissa of Fig. 1a at each temperature depends on the method of calculating D_{eff}. These values range from 1.05×10^{-3} to 1.25×10^{-3} at the peak temperature and thus a band of values for the pseudo-modulus is indicated in Fig. 1a. The value of C_s at the peak temperature is deter-

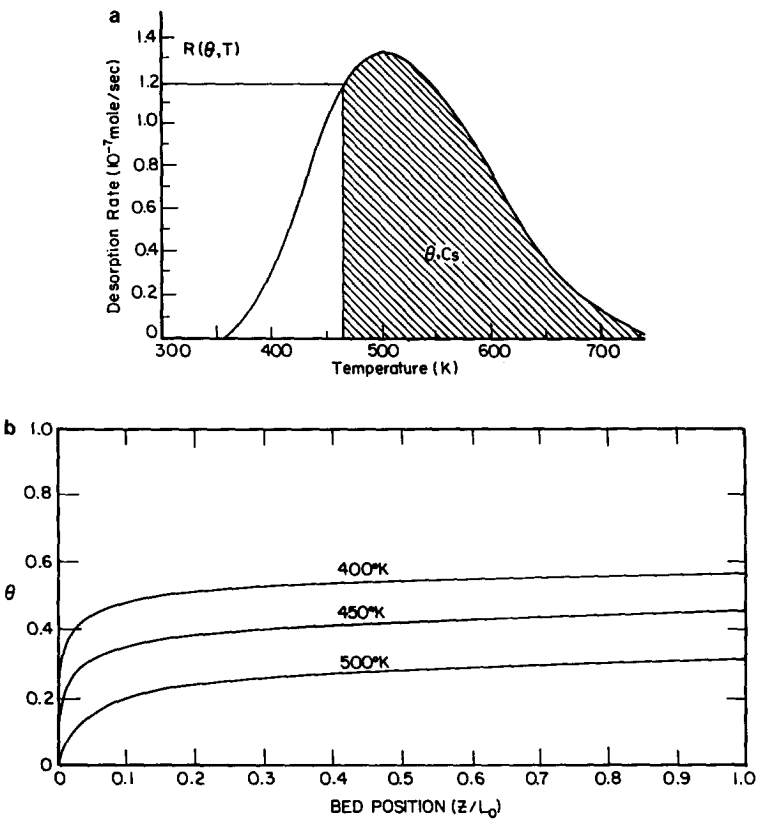

FIG. 3. (a) Experimental desorption spectrum of H_2 from an initial coverage of 0.7 from Ni/SiO_2 and (b) the surface phase H_2 profile down the axial length of the bed during TPD (*4*).

mined as the cross-hatched area (Fig. 2a). The total area under the TPD spectrum is proportional to C_m, which for the catalyst was determined to be 8.5×10^{-4} to 9.7×10^{-4} mol/cm^3 based on H_2 chemisorption. We assume a stoichiometry of CO/Ni = 0.5 although other values have been reported (*4*). Applying the results presented in Table 2 to the characteristic plot shown in Fig. 1a we find that $\eta > 0.99$, which indicates negligible internal concentration gradients within the catalyst particles.

Second-Order Desorption of H_2

Figure 3a is a TPD spectrum of H_2 desorption for an initial coverage of 0.7 from Ni/SiO_2. Figure 3b is the analog to Fig. 2b and demonstrates that here also axial dispersion is negligible and thus the axial concentration of adsorbate in the bed is uniform throughout the TPD experiment (*5*).

Following the procedures outlined above for first-order desorption the value of η at the peak temperature is found from the results of Fig. 1b to be $\eta \gg 0.99$.

DISCUSSION

Two attempts have been made to define criteria for the absence of intraparticle mass transfer effects during TPD in the presence of readsorption. Ibok and Ollis (*7*) have proposed that these effects, when desorption is first order, will be negligible provided the following relationship is satisfied,

$$r_s < \left[\left(\frac{D_{eff}}{1+K}\right)\frac{C_s|_{T_m}}{k\nu_m R|_{T_m}}\right]^{1/2}. \qquad (8)$$

This relationship was derived by modification of the Weisz–Prater (*1*) criterion, which was developed for *isothermal* reaction conditions. There exists considerable discussion in the literature (*16, 17*) regarding the applicability of their criterion to a TPD process. We have used this criterion to calculate the maximum particle size allowable to avoid intraparticle concentration gradients. The result yields an unreasonably small number ($<10^{-4}$ cm) for all the TPD cases considered here. This result is inconsistent with the experimental findings presented in the previous section. This inconsistency suggests that this criterion is either not applicable or overly restrictive.

Demmin and Gorte (*16*) have proposed, for the case of first-order desorption, design parameters for TPD from a packed bed of spherical particles. The results of their model are expressed in terms of six dimensionless groups. Each group provides an upper bound that should not be exceeded to allow the proper analysis of TPD curves. For example, they concluded that intraparticle concentration gradients are determined by the value of $Qr_s/4\pi r_s^2 N D_p$. Concentration gardients are significant if this parameter is greater than 0.05. They also concluded that some gradients will always exist in the particles at the bed entrance of a plug-flow reactor but the fraction of the bed for which this is important will be negligible when this parameter is small. They considered *only first-order desorption kinetics*. To assess the importance of intraparticle concentration gradients this parameter was evaluated for the CO TPD experiments of this study; H_2 TPD could not be analyzed. The results show that the value of this criterion is less than 0.05 (*16*) over the entire temperature range of desorption and thus intraparticle concentration gradients are predicted to be negligible. This calculation demonstrates that the criterion proposed by Demmin and Gorte provides a sound basis for predicting the onset of severe intraparticle mass transfer effects. This is also consistent with experimental findings.

TABLE 3

An Example in Which Significant Intraparticle Concentration Gradients Exist during the TPD Process

Catalyst	Platinum black
Surface area ($\times 10^{-3}$ cm^2/g)	1.25
Cross-sectional area of Pt atom (Å)	9
The order of desorption	Second order
Adsorbate	H_2
Carrier gas	N_2
Weight of catalyst (g)	2.54
Particle size (cm)	0.42
Bed volume (cm^3)	0.2
Temperature (K)	363
D_{eff}^{+} ($\times 10^{-3}$ cm^2/s)	3.1
D_{eff}^{++} ($\times 10^{-3}$ cm^2/s)	3.7
R ($\times 10^{-8}$ mol/cm^3)	1.19
θ	0.085
C_s ($\times 10^{-6}$ mol/cm^3)	1.2
$Rr_s^2/V_c D_{eff}$ ($\times 10^{-7}$)	7.1–8.5
η	0.75

A review of the TPD literature has shown that complete experimental conditions and/or results are often not given. One study, namely H_2 TPD from Pt black, has been reported. Table 3 lists the pertinent experimental values to serve as an example in which significant intraparticle concentration gradients exist during the TPD process. Several methods can be used to minimize this concentration gradient. For example, a decrease in particle size is an attractive direction to pursue. Using the data presented in Table 3 as an example, a factor of 2 decrease in particle size results in a factor of 4 decrease in the value of pseudo-modulus, and the resulting effectiveness factor increases from 0.75 to 0.90.

Our analysis demonstrates that *during* TPD in a flow geometry, where a small bed of catalyst particles is perfused by a flow of a carrier gas, numerous factors can determine the existence of intraparticle mass transfer effects. The experimentalist should be aware of these effects and design his experiment to avoid the possible complications that could arise in evaluating kinetic parameters from TPD spectra. Table 4 presents several factors that should be con-

TABLE 4

Impact of Design Parameters on the Effectiveness Factor

Factor	Variation	Effectiveness factor	Comment
R	Increase	Decrease	
C_s	Increase	Increase	
r_s	Increase	Decrease	
D_{eff}	Increase	Increase	
Vc	Increase (dilute with inert particles)	Depends on which dominates	(a) C_s decreases (b) Abscissa decreases
β	Increase	Depends on which dominates	(a) R increases (b) C_s decreases
α	Increase	Depends on which dominates	(a) C_s increases (b) R increases
m	Increase	Increase	

sidered in the design of a TPD experiment and how they impact on intraparticle mass transfer. The effect of these factors can be discussed qualitatively. For example, an increase in the initial coverage will increase η (all other experimentally controllable factors maintained constant) but will also increase R, the measured rate, which will generally decrease η. The actual effect on η depends on which factor is dominating in the system under study. Evaluation of the dominant factor requires experimental spectra and application of the procedures outlined in the previous section.

APPENDIX: NOMENCLATURE

R,R Observed reaction rate (mol/s).
V_c,Vc Bed volume (cm^3).
C_i Adsorbate concentration at the center of particle (mol/cm^3).
C_m Total concentration of surface sites accessible for adsorption (mol/cm^3).
C_0 Adsorbate concentration at the outer surface (mol/cm^3).
$C_p(0)$ Gas phase concentration of adsorbate at the center of the particles (mol/cm^3).
C_s Surface concentration of reactant (mol/cm^3).
D_{eff} Effective diffusion coefficient (cm^2/s).
D_m Molecular diffusivity (cm^2/s).
K Adsorption equilibrium constant.
k_a Adsorption rate constant (atm^{-1} s^{-1}).
k_d Desorption rate constant (1/s).
k_{eff} Effective desorption rate constant ((concentration)$^{1-n}$ s^{-1}).
m Catalyst mass (g).
n Order of the reaction.
P_a Gas phase pressure of the adsorbate (atm).
Q Flow rate of the carrier gas (cm^3/s).
T Temperature (K).
ϕ_s Thiele diffusion modulus for spherical catalyst particles.
r_s Catalyst particle radius (cm).
α $C_p(0)/C_s$.
β Heating rate (K/s).
η Effectiveness factor.
θ Surface coverage.
v_m Specific adsorption sites/cm^3 (moles of sites/cm^3).

APPENDIX

The mass balance describing the adsorbate concentration gradient within a spherical particle under quasi-steady-state conditions with readsorption is written as

$$\frac{d^2C}{dr^2} + \frac{2}{r}\frac{dC}{dr} + \frac{1}{D_{eff}}[k_d C^n - k_a P_a (C_m - C)^n] = 0 \quad \text{(A.1)}$$

with associated boundary conditions

$$\frac{dC}{dr}(r = 0) = 0 \quad \text{(A.2)}$$

$$C(r = r_s) = C_0. \quad \text{(A.3)}$$

This second-order differential equation, two-point boundary value problem, can be solved numerically using an iteration scheme described as the "shooting" method (*18*). Briefly, radial adsorbate concentration profiles are evaluated for sets of parameters: k_d, k_a, P_a, C_m, n, r_s, and C_0. Here C_0 is the concentration at the surface of the particle, namely at $r = r_s$. The concentration gradient at the particle surface is

evaluated numerically from the resulting concentration profile.

The value of C_0 "pins" the concentration profile, sets the value of C_i, and establishes the basis for numerically calculating the value of C_s, i.e., the average concentration of the adsorbate in the particle at T, which is

$$C_s = \frac{4\pi \int_0^{r_s} C_T(r) r^2 \, dr}{\frac{4}{3}\pi r_s^3}. \quad \text{(A.4)}$$

In Eq. (A.4) $C_T(r)$ is the concentration profile at temperature T and for a fixed set of parameter values. Values of C_s are presented in Figs. 1a and 1b.

The observed desorption rate is calculated by integrating the desorption/readsorption rate over the entire sphere using the local adsorbate concentration obtained from the numerical simulation,

$$R = 4\pi \int_0^{r_s} [k_d C_T(r)^n - k_a P_a (C_m - C_T(r))^n] r^2 \, dr. \quad \text{(A.5)}$$

The effectiveness factor η, defined as the ratio of the observed desorption rate to the desorption rate evaluated at the concentration at the center of particle, is

$$\eta = \frac{R}{[k_d C_i^n - k_a P_a (C_m - C_i)^n] V_c}. \quad \text{(A.6)}$$

The modulus for the desorption process, ϕ_s, is evaluated as

$$\phi_s = \frac{r_s}{3}\left[\frac{k_{eff} C_i^{n-1}}{D_{eff}}\right]^{1/2} = \frac{r_s}{3}\left[\frac{k_d C_i^n - k_a P_a (C_m - C_i)^n}{C_i D_{eff}}\right]^{1/2}. \quad \text{(A.7)}$$

The product of η and ϕ_s^2 yields

$$\eta\phi_s^2 = R \frac{r_s^2}{9 V_c C_i D_{eff}} \quad \text{(A.8)}$$

and rearrangement of Eq. (A.8) yields

$$9\eta\phi_s^2 C_i = \frac{R r_s^2}{V_c D_{eff}}. \quad \text{(A.9)}$$

Numerically, the left-hand side of Eq. (A.9) is evaluated employing the same parameters as those used to generate the adsorbate concentration profile. Contour plots of η vs $Rr_s^2/V_c D_{eff}$ (i.e., $9\eta\phi_s^2 C_i$) parametric in C_s were constructed using different sets of parameters described earlier and are presented in Fig. 1.

ACKNOWLEDGMENT

This work was supported by the Division of Chemical Sciences, Office of Basic Energy Research under the Department of Energy Grant DE-FG02-87ER-13650.

REFERENCES

1. Weisz, P. J., and Prater, C. D., *Adv. Catal.* **6,** 143 (1954).
2. Smith, J. M., "Chemical Engineering of Kinetics," 2nd ed., p. 478. McGraw–Hill, New York, 1970.
3. Gorte, R. J., *J. Catal.* **75,** 164 (1982).
4. Lee, P. I., Schwarz, J. A., and Heydweiller, J. C., *Chem. Eng. Sci.* **4**(3), 509 (1985).
5. Lee, P. I., and Schwarz, J. A., *J. Catal.* **73,** 272 (1982).
6. Rieck, J. S., and Bell, A. T., *J. Catal.* **85,** 143 (1984).
7. Ibok, E. E., and Ollis, D. F., *J. Catal.* **66,** 391 (1980).
8. Herz, C. H., Kiela, J. B., and Martin, S. P., *J. Catal.* **73,** 66 (1982).
9. Lee, P.-I., Huang, Y.-J., Schwarz, J. A., and Heydweiller, J. C., submitted for publication.
10. Falconer, J. L., and Schwarz, J. A., *J. Catal. Rev. Sci. Eng.* **25**(2), 141 (1983).
11. Fuller, E. N., Schettler, P. D., and Giddings, J. C., *Ind. Eng. Chem.* **58**(5), 19 (1966).
12. Hirschfelder, J. O., Curtiss, C. F., and Bird, R. B., "Molecular Theory of Gas and Liquids." Wiley, New York, 1954.
13. Slattery, J. C., and Bird, R. B., *AIChE J.* **4,** 137 (1958).
14. Gilliland, E. R., *Ind. Eng. Chem.* **26,** 681 (1934).
15. Huang, Y.-J., and Schwarz, J. A., *J. Catal.* **99,** 249 (1986).
16. Demmin, R. A., and Gorte, R. J., *J. Catal.* **90,** 32 (1984).
17. Criado, J. M., Malet, Pilar, Munuera, G., and Rives-Arnau, V., *J. Catal.* **75,** 4228 (1982).
18. Robets, C. E., Jr., "Ordinary Differential Equations," Chap. 10. Prentice–Hall, Englewood Cliffs, NJ, 1979.